Organometallics 1994, 13, 1294-1299

Synthesis and Structural Characterization of $[Cr(t\text{-}C_4H_9HNC{\equiv}CNH\text{-}t\text{-}C_4H_9)(CN\text{-}t\text{-}C_4H_9)_4I]I$. Reductive Coupling of Isocyanide Ligands in a First Row Transition Metal Complex

Jacqueline A. Acho and Stephen J. Lippard*

Department of Chemistry, Massachusetts Institute of Technology, Cambridge, Massachusetts 02139

Received November 10, 1993[⊗]

The reductive coupling of two isocyanide ligands to form a coordinated bis(alkylamino)acetylene molecule, previously known for $[M(CNR)_6]$ complexes, M = Mo, W and R = alkyl, has been extended to include the first row transition metal chromium. An improved synthesis and X-ray structure determination of the known precursor molecule, $[Cr(CN\text{-}t\text{-}C_4H_9)_6]$ (**1**), are reported. Crystal data for **1**: monoclinic $P2_1$, $a = 17.688(6)$ Å, $b = 11.912(1)$ Å, $c = 19.221(6)$ Å, $\beta = 116.65(1)°$, $Z = 4$. The structure was solved by conventional direct methods and refined by full matrix least squares to $R = 0.060$ and $R_w = 0.070$ for 4851 reflections with $I \geq 3\sigma(I)$. The coordination geometry is approximately octahedral. A noteworthy feature of the structure is the variability of isocyanide C–N–C bend angles [136.1(9)–175(1)°], which correlate linearly with the M–C bond lengths for M = Cr and Mo. Addition of 2 equiv of HI(aq) to $[Cr(CN\text{-}t\text{-}C_4H_9)_6]$ in THF resulted in carbon–carbon bond formation between two isocyanide ligands to afford $[Cr(t\text{-}C_4H_9HNC{\equiv}CNH\text{-}t\text{-}C_4H_9)(CN\text{-}t\text{-}C_4H_9)_4I]I$ (**2**), which has been characterized by ^1H and $^{13}C\{^1H\}$ NMR and IR spectroscopic, as well as elemental, analyses. The solid-state structure of **2**·(toluene) was determined in a single crystal X-ray diffraction study. Crystal data for **2**·(toluene): monoclinic $P2_1/n$, $a = 15.927(4)$ Å, $b = 17.397(2)$ Å, $c = 17.351(4)$ Å, $\beta = 111.36(1)°$, $Z = 4$. The structure was solved by direct methods and refined by full matrix least-squares procedures to $R = 0.035$ and $R_w = 0.042$ for 5523 reflections with $I \geq 3\sigma(I)$. The idealized geometry about the chromium center in **2** is C_{2v} capped trigonal prismatic. Reaction of **2** with excess H_2O_2 resulted in the oxidative removal of the coupled acetylene as *N,N'*-di-*tert*-butyloxamide.

Introduction

Following the discovery of the reductive coupling of two isocyanide ligands in $[Mo(CN\text{-}t\text{-}C_4H_9)_6I]I$,[1] much work has been carried out to explore the generality of the reaction and to elucidate the mechanism of carbon–carbon bond formation.[2,3] Work from our laboratory extended the reductive coupling chemistry both to CO complexes and to group V transition metals. Reductive coupling of CO ligands, originally studied with niobium and tantalum, was recently achieved with vanadium with two unexpected results.[4] Not only was the coupled acetylene ligand more readily removed from the metal than in the case of the Nb and Ta analogs, but also the smaller vanadium center afforded an unprecedented 6-coordinate cation, $[V(Me_3SiOC{\equiv}COSiMe_3)(dmpe)_2]^+$ (eq 1).

$$\mathrm{Na[V(CO)_2(dmpe)_2]} \xrightarrow{2\mathrm{Me_3SiOTf}} \mathrm{[V(Me_3SiOC{\equiv}COSiMe_3)(dmpe)_2]OTf} \qquad (1)$$

Given these differences between the chemistry of a first row transition metal complex compared to second and third row group V transition metal complexes, we were interested in extending the reductive coupling of group VI Mo and W isocyanide complexes to the first row congener Cr. Reductive coupling of isocyanides on group VI metal centers is well precedented for the second and third row metals.[1,3,5–10] The reaction was first discovered during a study of 7-coordinate molybdenum isocyanide complexes. Refluxing a solution of $[Mo(CN\text{-}t\text{-}C_4H_9)_6I]I$ in slightly wet THF overnight in the presence of zinc dust

$$\mathrm{[Mo(CNR)_6I]^+} \xrightarrow[\mathrm{THF}]{\mathrm{Zn}} \mathrm{[Mo(CNR)_6]} \xrightarrow{\mathrm{HX}} \mathrm{\{[Mo({\equiv}CNHR)(CNR)_5]X\}} \xrightarrow{\mathrm{HX}} \mathrm{[Mo(RHNC{\equiv}CNHR)(CNR)_4X]X} \qquad (2)$$

R = alkyl; X = halide, triflate

produced the coupled product $[Mo(t\text{-}C_4H_9HNC{\equiv}CNH\text{-}t\text{-}C_4H_9)(CN\text{-}t\text{-}C_4H_9)_4I]I$.[1] Subsequent mechanistic studies revealed that the reaction pathway, shown in eq 2,[6] involves reduction of the $[Mo(CNR)_6I]^+$ cation first to afford the

---

[⊗] Abstract published in *Advance ACS Abstracts*, February 15, 1994.

(1) Lam, C. T.; Corfield, P. W. R.; Lippard, S. J. *J. Am. Chem. Soc.* **1977**, *99*, 617.

(2) Carnahan, E. M.; Protasiewicz, J. D.; Lippard, S. J. *Acc. Chem. Res.* **1993**, *26*, 90.

(3) Vrtis, R. N.; Lippard, S. J. *Isr. J. Chem.* **1990**, *30*, 331.

(4) Protasiewicz, J. D.; Lippard, S. J. *J. Am. Chem. Soc.* **1991**, *113*, 6564.

(5) Giandomenico, C. M.; Lam, C. T.; Lippard, S. J. *J. Am. Chem. Soc.* **1982**, *104*, 1263.

(6) Carnahan, E. M.; Lippard, S. J. *J. Chem. Soc., Dalton Trans.* **1991**, 699.

(7) Caravana, C.; Giandomenico, C. M.; Lippard, S. J. *Inorg. Chem.* **1982**, *21*, 1860.

(8) Filippou, A. C.; Grünleitner, W.; Völkl, C.; Kiprof, P. *Angew. Chem., Int. Ed. Engl.* **1991**, *30*, 1167.

(9) Filippou, A. C.; Völkl, C.; Grünleitner, W.; Kiprof, P. *J. Organomet. Chem.* **1992**, *434*, 201.

(10) Fraústo da Silva, J. J. R.; Pellinghelli, M. A.; Pombeiro, A. J. L.; Richards, R. L.; Tiripicchio, A.; Wang, Y. *J. Organomet. Chem.* **1993**, *454*, C8.

0276-7333/94/2313-1294$04.50/0

homoleptic Mo^0 isocyanide complex, [Mo(CNR)$_6$], which was isolated as a discrete intermediate. Addition of 1 equiv of acid transformed this compound to a metal (alkylamino)carbyne complex which, although not isolated, was postulated to exist by analogy to reactions carried out with silylating agents instead of HX.[6] Addition of a second equivalent of HX triggered C—C bond formation, yielding the metal-bound acetylene complex, [Mo(RHNC$\equiv$CNHR)(CNR)$_4$X]X. Since the chromium analog of [Mo(CNR)$_6$] for R = *t*-C$_4$H$_9$, [Cr(CN-*t*-C$_4$H$_9$)$_6$], is a known compound,[11,12] we wondered whether it might be possible to couple the isocyanide ligands in this molecule by similar chemistry. To do so would not only extend the reaction to a new metal center but would also provide a powerful test of the generality of the reaction mechanism. Moreover, since among the few homoleptic isocyanide complexes of Cr(0) X-ray crystal structures are available only for two aryl isocyanide complexes, [Cr(CNPh)$_6$][13] and [Cr{CN[2,6-(*i*-Pr)$_2$Ph]}$_6$],[14] and just one alkyl isocyanide, [Cr(CNCF$_3$)$_6$],[15] we also carried out an X-ray diffraction study of 1. This information allows an examination of geometric factors that might relate to its propensity to undergo reductive coupling. Information of this kind was valuable in understanding the reactivity of [Mo(CN-*t*-C$_4$H$_9$)$_6$].[6] Knowledge of the structure also helps to assess the changes that take place upon reductive coupling of two adjacent ligands in 1.

Experimental Section

General Procedures. All manipulations were carried out in a Vacuum Atmospheres nitrogen-filled drybox or by using standard Schlenk line techniques. Solvents were distilled under nitrogen. Tetrahydrofuran (THF), toluene, and pentane were distilled from sodium benzophenone ketyl. NMR spectra were obtained on a Varian XL-300 spectrometer at room temperature. IR spectra were recorded on a Bio-Rad FTS7 Fourier transform instrument. GC/MS studies were performed on a 12-m Hewlett-Packard Model 5971 A system with a fluid phase methylsilicone column. The yield was determined by comparison to an internal standard (naphthalene).

Materials. *tert*-Butyl isocyanide, CrCl$_2$, and H$_2$O$_2$ (30%) were purchased from commercial vendors and used without further purification. Hydriodic acid (HI, 57%) was deoxygenated prior to use by purging the solution with argon for 10 min.

Synthesis. [Cr(CN-*t*-C$_4$H$_9$)$_6$] (1). The preparation of [Cr(CN-*t*-C$_4$H$_9$)$_6$], a known compound,[11,12] was carried out as previously reported for [Mo(CN-*t*-C$_4$H$_9$)$_6$][6] with minor changes. To a suspension of CrCl$_2$ (139 mg, 1.13 mmol) in 20 mL of THF was added excess 1% Na/Hg amalgam (29.8 g of Hg, 0.302 g, 13.1 mmol of Na) and CN-*t*-C$_4$H$_9$ (566 mg, 6.81 mmol). The reaction mixture was stirred vigorously for 3 h in the absence of light. The green-yellow solution was decanted from the amalgam and filtered through silica gel. The solvent was removed from the orange-brown filtrate in vacuo, and the resulting solid was extracted into 50 mL of pentane. Evaporation of the pentane left 430 mg (69%) of bright orange air- and light-sensitive product which could be recrystallized from pentane to give an orange crystalline product. IR (pentane): 2955 (w), 2088 (sh), 1953 (sh), 1919 (sh), 1883 (vs, br), 1842 (sh), 1390 (w), 1361 (m), 1211 (m) cm^{-1}. ^{1}H NMR (C$_6$D$_6$): 1.35 ppm (s). Anal. Calcd for C$_{30}$H$_{54}$N$_6$Cr: C, 65.42; H, 9.88; N, 15.26. Found: C, 65.50; H, 10.01; N, 15.28.

Table 1. X-ray Crystallographic Information for [Cr(CN-*t*-C$_4$H$_9$)$_6$] (1) and [Cr(*t*-C$_4$H$_9$HNC$\equiv$CNH-*t*-C$_4$H$_9$)(CN-*t*-C$_4$H$_9$)$_4$I]I·(toluene) (2·(toluene))[a]

	1	2·(toluene)
formula	C$_{30}$H$_{54}$N$_6$Cr	C$_{37}$H$_{64}$N$_6$I$_2$Cr
mol wt	550.8	898.8
a, Å	17.688(6)	15.927(4)
b, Å	11.912(1)	17.397(2)
c, Å	19.221(6)	17.351(4)
β, deg	116.65(1)	111.36(1)
V, Å^3	3619(2)	4477(2)
T, °C	−71.7	−71.7
Z	4	4
ρ_{calc}, g/cm^{-3}	1.011	1.333
space group	$P2_1$	$P2_1/n$
2θ limits, deg	3–54	3–50
data limits	$+h,+k,\pm l$	$+h,+k,\pm l$
μ, cm^{-1}	3.303	16.42
total no. of data	8280	8663
no. of unique data[b]	4851	5523
no. of params	657	415
p factor	0.03	0.03
R[c]	0.060	0.035
R_w	0.070	0.042

[a] Data were collected on an Enraf-Nonius CAD-4F kappa geometry diffractometer using Mo Kα radiation. [b] Observation criterion $I > 3\sigma(I)$. [c] $R = \sum||F_o| - |F_c||/\sum|F_o|$, $R_w = [\sum w(|F_o| - |F_c|)^2/\sum w|F_o|^2]^{1/2}$, where $w = 1/\sigma^2(F)$, as defined in: Carnahan, E. M.; Rardin, R. L.; Bott, S. G.; Lippard, S. J. *Inorg. Chem.* **1992**, *31*, 5193.

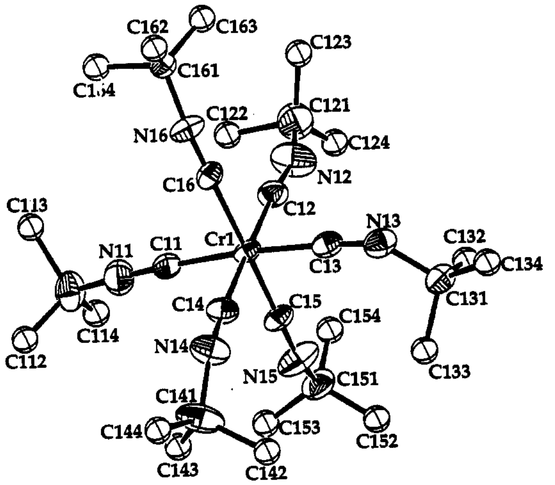

Figure 1. ORTEP diagram of one of the two molecules of [Cr(CN-*t*-C$_4$H$_9$)$_6$] (1) in the crystallographic asymmetric unit, showing the atom labeling scheme and the 40% probability thermal ellipsoids. The second molecule contains the atoms Cr2, C21, N21, C211, etc. The methyl carbons of the *tert*-butyl groups are displayed as 3-Å^2 isotropic spheres for clarity.

[Cr(*t*-C$_4$H$_9$HNC$\equiv$CNH-*t*-C$_4$H$_9$)(CN-*t*-C$_4$H$_9$)$_4$I]I (2). To a bright orange solution of [Cr(CN-*t*-C$_4$H$_9$)$_6$] (200 mg, 0.363 mmol) in 15 mL of THF was added 2 equiv of aqueous HI (57%, 109 μL, 0.729 mmol). The solution immediately turned brown. After stirring for 1 h, the solution was passed through a 1-in. pad of silica. The solvent was evaporated and the red-brown product was washed with several portions of pentane, and 252 mg (0.312 mmol, 86%) of 2 was collected on a fritted funnel. The product was judged to be >95% pure by ^{1}H NMR spectroscopy and could be further purified by recrystallization from THF at −30 °C. IR (KBr): 3151 (m), 3106 (m), 2978 (s), 2121 (br, vs), 1608 (vs), 1520 (m), 1464 (s), 1369 (s), 1203 (vs), 1034 (w), 728 (w), 584 (m), 554 (m) cm^{-1}. ^{1}H NMR (CDCl$_3$): δ 10.51 (br, N*H*), 1.74 (s, *t*-C$_4$*H*$_9$-NHCCNH-*t*-C$_4$*H*$_9$), 1.44 (s, CN-*t*-C$_4$*H*$_9$) ppm. ^{13}C{^{1}H} NMR (CDCl$_3$): δ 30.1 (C(*C*H$_3$)$_3$), 31.1 (C(*C*H$_3$)$_3$), 56.2 (*C*(CH$_3$)$_3$), 56.8 (*C*(CH$_3$)$_3$), 168.1 (M—C), 208.9 (C$\equiv$C) ppm. Anal. Calcd for C$_{30}$H$_{56}$N$_6$I$_2$Cr: C, 44.67; H, 7.00; N, 10.42. Found: C, 44.63; H, 6.92; N, 10.24.

Reaction of [Cr(*t*-C$_4$H$_9$HNC$\equiv$CNH-*t*-C$_4$H$_9$)(CN-*t*-C$_4$H$_9$)$_4$I]I (2) with H$_2$O$_2$: Removal of the Coupled Ligand as *N,N'*-Di-*tert*-butyloxamide. A solution of 0.074 g (0.091 mmol) of

---

(11) Timms, P. L.; Turney, T. W. *J. Chem. Soc., Dalton Trans.* **1976**, 2021.

(12) Chiu, K. W.; Howard, C. C.; Wilkinson, G.; Galas, A. M. R.; Hursthouse, M. B. *Polyhedron* **1982**, *1*, 803–808.

(13) Ljungström, E. *Acta Chem. Scand., Ser. A* **1978**, *A32* (1), 47–50.

(14) Anderson, K. A.; Scott, B.; Wherland, S.; Willett, R. D. *Acta Crystallogr., Sect. C: Cryst. Struct. Commun.* **1991**, *C47* (11), 2337–2339.

(15) Lentz, D. *J. Organomet. Chem.* **1990**, *381*, 205.

Table 2. Final Positional Parameters for $[Cr(CN\text{-}t\text{-}C_4H_9)_6]$ (1)[a]

atom	x	y	z	B_{eq}, Å^2 [b]	atom	x	y	z	B_{eq}, Å^2 [b]
Cr1	0.78923(8)	0.1764	0.51317(8)	2.69(3)	C151	0.5304(6)	0.169(1)	0.4872(6)	4.9(3)
Cr2	0.79466(8)	0.4081(1)	0.00710(7)	2.64(3)	C152	0.4668(8)	0.092(2)	0.443(1)	12.4(6)
N11	0.8169(5)	0.3278(8)	0.6571(5)	5.2(2)	C153	0.528(1)	0.199(2)	0.562(1)	13.7(7)
N12	0.7085(6)	0.3737(8)	0.3989(6)	6.2(3)	C154	0.513(1)	0.272(2)	0.439(1)	14.8(8)
N13	0.7360(5)	0.0208(7)	0.3711(5)	4.2(2)	C161	1.0193(5)	0.3428(9)	0.5145(5)	3.7(2)
N14	0.8554(6)	−0.0292(7)	0.6207(5)	5.0(2)	C162	1.0961(7)	0.282(1)	0.5246(8)	8.4(4)
N15	0.6137(5)	0.1354(8)	0.5041(6)	6.1(2)	C163	0.9818(9)	0.407(2)	0.442(1)	11.9(6)
N16	0.9587(4)	0.2689(6)	0.5212(4)	4.3(2)	C164	1.047(1)	0.424(1)	0.5836(9)	10.4(5)
N21	0.7262(5)	0.2195(7)	−0.1143(5)	3.8(2)	C211	0.6443(5)	0.1660(8)	−0.1612(5)	4.0(2)
N22	0.7078(6)	0.5819(8)	−0.1233(5)	5.5(2)	C212	0.5820(7)	0.255(1)	−0.2051(7)	7.9(4)
N23	0.8550(6)	0.5916(8)	0.1392(5)	4.5(2)	C213	0.6205(9)	0.105(1)	−0.1065(8)	8.3(4)
N24	0.8558(5)	0.2335(7)	0.1401(5)	4.9(2)	C214	0.6545(7)	0.086(1)	−0.2168(6)	6.2(3)
N25	0.9607(5)	0.4786(6)	−0.0024(4)	4.2(2)	C221	0.6889(6)	0.7039(8)	−0.1351(6)	4.7(2)
N26	0.6245(5)	0.3910(8)	0.0126(5)	5.8(2)	C222	0.728(1)	0.747(2)	−0.186(1)	5.8(5)
C11	0.8090(5)	0.2695(8)	0.6030(5)	3.6(2)	C223	0.723(1)	0.763(2)	−0.054(1)	5.2(4)
C12	0.7397(6)	0.3025(8)	0.4442(6)	3.8(2)	C224	0.590(1)	0.721(2)	−0.183(1)	5.5(5)
C13	0.7595(6)	0.0831(8)	0.4266(6)	3.5(2)	C231	0.8832(6)	0.666(1)	0.2038(6)	4.6(2)
C14	0.8332(6)	0.0509(9)	0.5806(6)	3.7(2)	C232	0.954(1)	0.727(2)	0.213(1)	21(1)
C15	0.6812(5)	0.1507(8)	0.5074(5)	3.5(2)	C233	0.811(1)	0.737(2)	0.195(1)	17.6(8)
C16	0.8961(5)	0.2321(7)	0.5188(5)	3.3(2)	C234	0.907(1)	0.594(2)	0.2752(9)	13.0(6)
C21	0.7551(5)	0.2930(7)	−0.0685(5)	2.8(2)	C241	0.8276(7)	0.173(1)	0.1921(7)	5.7(3)
C22	0.7428(6)	0.5172(8)	−0.0715(6)	3.4(2)	C242	0.895(1)	0.096(2)	0.242(1)	12.8(6)
C23	0.8314(6)	0.5251(8)	0.0899(6)	3.4(2)	C243	0.747(1)	0.110(2)	0.1373(9)	13.3(6)
C24	0.8366(5)	0.2983(8)	0.0891(6)	3.2(2)	C244	0.801(1)	0.258(1)	0.234(1)	10.7(6)
C25	0.9010(5)	0.4452(7)	0.0015(5)	3.4(2)	C251	1.0279(5)	0.5507(9)	−0.0001(6)	4.5(2)
C26	0.6891(5)	0.3998(8)	0.0105(5)	3.2(2)	C252	0.993(1)	0.659(2)	−0.033(1)	6.1(5)
C111	0.8085(7)	0.404(1)	0.7109(6)	5.4(3)	C253	1.071(1)	0.489(2)	−0.044(1)	3.4(3)
C112	0.8431(9)	0.352(1)	0.7900(7)	8.4(4)	C254	1.095(1)	0.545(2)	0.092(1)	4.8(4)
C113	0.871(1)	0.502(1)	0.719(1)	12.6(6)	C261	0.5556(7)	0.440(1)	0.0234(7)	5.5(3)
C114	0.7220(9)	0.435(2)	0.688(1)	16.4(7)	C262	0.516(2)	0.361(2)	0.055(1)	5.5(5)
C121	0.6781(7)	0.480(1)	0.3689(7)	5.8(3)	C263	0.598(1)	0.545(2)	0.082(1)	4.4(4)
C122	0.698(2)	0.550(2)	0.442(2)	23(1)	C264	0.487(2)	0.498(3)	−0.060(2)	7.4(7)
C123	0.729(1)	0.526(1)	0.332(1)	13.4(7)	C222B	0.771(2)	0.760(3)	−0.126(2)	9.7(8)
C124	0.593(1)	0.483(3)	0.323(2)	28(1)	C223B	0.613(3)	0.725(4)	−0.126(2)	12(1)
C131	0.6598(6)	−0.0449(8)	0.3250(5)	4.1(2)	C224B	0.640(2)	0.722(3)	−0.232(2)	9.5(8)
C132	0.5899(7)	0.041(1)	0.2784(7)	6.8(3)	C252B	0.986(2)	0.622(3)	−0.084(2)	8.4(7)
C133	0.6363(7)	−0.112(1)	0.3803(6)	6.6(3)	C253B	1.109(2)	0.488(3)	0.008(2)	9.4(8)
C134	0.6768(7)	−0.121(1)	0.2717(6)	5.4(3)	C254B	1.051(2)	0.638(2)	0.065(1)	7.7(6)
C141	0.8337(9)	−0.103(1)	0.6692(8)	6.7(4)	C262B	0.559(2)	0.366(2)	0.099(1)	7.1(6)
C142	0.771(1)	−0.193(2)	0.617(1)	14.6(7)	C263B	0.539(3)	0.553(4)	0.016(3)	15(1)
C143	0.781(2)	−0.037(1)	0.699(1)	16.6(9)	C264B	0.474(2)	0.401(3)	−0.048(2)	10.4(8)
C144	0.912(1)	−0.155(2)	0.730(1)	14.5(7)					

[a] Numbers in parentheses are errors in the last significant figure. See Figure 1 for the atom labeling scheme. [b] $B_{eq} = {}^4/_3[a^2\beta_{11} + b^2\beta_{22} + c^2\beta_{33} + 2ab\cos(\gamma)\beta_{12} + 2ac\cos(\beta)\beta_{13} + 2bc\cos(\alpha)\beta_{23}]$.

Table 3. Selected Interatomic Bond Distances (Å) and Angles (deg) for $[Cr(CN\text{-}t\text{-}C_4H_9)_6]$ (1)[a]

	Bond Distances		
Cr1–C11	1.95(1)	Cr2–C21	1.89(1)
Cr1–C12	1.93(1)	Cr2–C22	1.89(1)
Cr1–C13	1.87(1)	Cr2–C23	1.99(1)
Cr1–C14	1.90(1)	Cr2–C24	1.92(1)
Cr1–C15	1.889(9)	Cr2–C25	1.980(8)
Cr1–C16	1.961(8)	Cr2–C26	1.900(7)
mean C–N	1.18(2)[b]	range C–N	1.16(1)–1.21(1)
mean N–C(Bu^t)	1.45(3)[b]	range N–C(Bu^t)	1.40(1)–1.49(1)
mean C–C(Me)	1.52(7)[b]	range C–C(Me)	1.36(2)–1.67(3)
	Bond Angles		
mean *cis* C–Cr–C	90(4)[b]	range *cis* C–Cr–C	84.5(4)–99.8(4)
mean *trans* C–Cr–C	173(3)[b]	range *trans* C–Cr–C	169.5(4)–177.5(4)
mean Cr–C–N	176(2)[b]	range Cr–C–N	172.9(8)–179.6(8)
C11–N11–C111	168(1)	C21–N21–C211	139.2(8)
C12–N12–C121	160(1)	C22–N22–C221	139(1)
C13–N13–C131	136.1(9)	C23–N23–C231	175(1)
C14–N14–C141	144(1)	C24–N24–C241	145(1)
C15–N15–C151	153(1)	C25–N25–C251	163.0(9)
C16–N16–C161	162.7(9)	C26–N26–C261	151(1)

[a] See footnote *a*, Table 2. [b] Numbers in parentheses are the standard deviations of the mean.

$[Cr(t\text{-}C_4H_9HNC{\equiv}CNH\text{-}t\text{-}C_4H_9)(CN\text{-}t\text{-}C_4H_9)_4I]I$ (**2**) in 10 mL of THF was prepared. To the stirred brown solution was added 10 equiv of H_2O_2 (30 μL, 0.98 mmol). The reaction was allowed to stir for 14 h and then filtered to remove a thin layer of fine brown precipitate. The orange filtrate was analyzed by GC/MS and found to contain *N*,*N'*-di-*tert*-butyloxamide (M^+ = 200) in 28% yield.

X-ray Structure Determinations of $[Cr(CN\text{-}t\text{-}C_4H_9)_6]$ (1) and $[Cr(t\text{-}C_4H_9HNC{\equiv}CNH\text{-}t\text{-}C_4H_9)(CN\text{-}t\text{-}C_4H_9)_4I]I\cdot$(toluene) (2·(toluene)). Bright orange crystals of **1** were grown by cooling to −30 °C a concentrated solution in pentane in the dark. The crystals were transferred to a cold stage and a block-shaped specimen of dimensions 0.2 × 0.3 × 0.4 mm was mounted on the tip of a quartz fiber with silicone grease. Study on the diffractometer at −72 °C indicated a primitive monoclinic cell. The crystal quality was judged to be acceptable on the basis of open counter ω-scans of several low angle reflections ($\Delta\bar{\omega}_{1/2}$ = 0.23°, no fine structure) and of axial photographs. A shroud was draped over the diffractometer to exclude room light. The unit cell parameters and intensity data were obtained by methods common in our laboratory,[16] details of which are provided in Table 1. Systematic absences and intensity statistics indicated the acentric space group $P2_1$, a choice later confirmed by the structure solution. The chromium atoms of the two molecules in the asymmetric unit were located by direct methods. The remaining non-hydrogen positions were determined by subsequent iterative least-squares refinements and difference Fourier maps. Most non-hydrogen atoms were refined anisotropically. Rotational disorder of methyl carbons on three of the *tert*-butyl groups resulted in high B_{eq} values. A two-site model for the methyl carbon atoms on these *tert*-butyl groups was introduced with 50% occupancy and isotropic temperature factors. All hydrogen atoms were placed in calculated positions and fixed to the attached carbon atoms (d_{C-H} = 0.95 Å, B_H = $1.2B_C$). The

---

[16] Carnahan, E. M.; Rardin, R. L.; Bott, S. G.; Lippard, S. J. *Inorg. Chem.* **1992**, *31*, 5193.

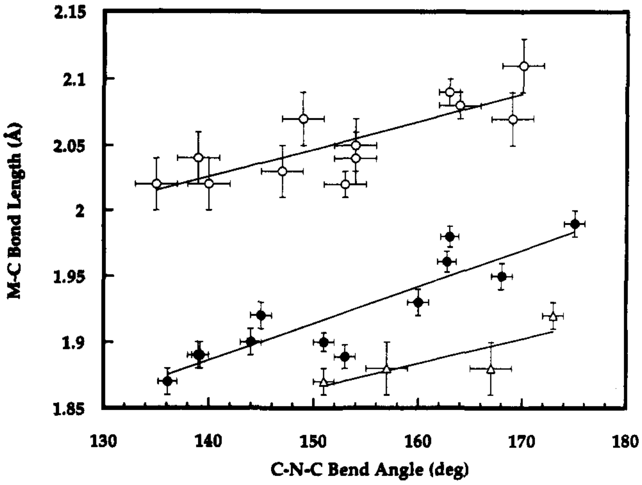

Figure 2. Plot of the isocyanide ligand C–N–C bend angle versus the M–C bond length for [Mo(CN-t-C_4H_9)$_6$] (open circles), [Cr(CN-t-C_4H_9)$_6$] (1) (filled circles), and [Cr-($CNCF_3$)$_6$] (triangles). Solid lines represent the best least squares fit to a linear relationship. Error bars denote ±1 esd.

enantiomorph reported is that which refined to the lower R_w value. The largest residual peak in the final difference Fourier map was 0.39 e/Å^3, located at a distance of 0.82 Å from C223.

Deep red-brown crystals of 2·(toluene) were grown by slowly cooling a warm saturated solution in toluene to −30 °C. The crystals were coated in Exxon Paratone-N, and an irregularly shaped specimen of dimensions 0.2 × 0.3 × 0.4 mm was frozen on the tip of a quartz fiber in a cold stream of N_2 at −72 °C. Preliminary studies indicated a primitive monoclinic cell. The crystal quality was judged to be acceptable on the basis of open counter ω-scans of several low angle reflections ($\Delta\bar{\omega}_{1/2}$ = 0.24°) and on axial photographs. The unit cell parameters and intensity data were obtained by methods standard in our laboratory,[16] details of which are provided in Table 1. An empirical ψ-scan absorption correction was applied to the data. Systematic absences and intensity statistics were consistent with the centrosymmetric space group $P2_1/n$. The two iodine atoms and the chromium atom were located by direct methods. The remaining non-hydrogen atoms were located by subsequent iterative least-squares refinements and difference Fourier maps. All non-hydrogen atoms were refined anisotropically. Hydrogen atoms H1 and H2 of the protonated bis(alkylamino)acetylene ligand were located on a difference Fourier map. Other hydrogen atoms were calculated and fixed on the attached carbon atoms (d_{C-H} = 0.95 Å, B_H = 1.2B_C). The largest residual peak in the final difference Fourier map was 1.18 e/Å^3, at a distance of 0.96 Å from the I2 anion.

Results and Discussion

The preparation of [Cr(CN-t-C_4H_9)$_6$] (1) reported here is more convenient and less expensive than earlier syntheses. The compound was first made from [Cr(C_8H_8)$_3$],[11] which is obtained by metal atom vapor techniques. It was later reported that red-brown crystals of 1 could be obtained in 24 hours by reducing [$Cr_2(O_2CCH_3)_4$] with sodium amalgam in the presence of excess *tert*-butyl isocyanide.[12] We found that the homoleptic compound 1 could be readily synthesized by the procedure reported previously for [Mo(CN-t-C_4H_9)$_6$].[6] The reduction of $CrCl_2$ by 1% sodium amalgam in THF in the presence of approximately 6 equiv of *tert*-butyl isocyanide afforded good yields of the bright orange product 1 (eq 3). The photosensitivity of 1 was noticed both in solution and in the crystalline state, for the bright orange color darkens to red-brown over several hours when the compound is exposed to light. The low C≡NR stretching frequency (1883 cm^{-1}) in the solution IR spectrum of 1 suggested a highly electron-dense metal center and considerable π-back-donation, indicating the compound to be a good candidate for the reductive coupling reaction.[3] The presumed π-back-bonding was corroborated by the X-ray structure determination.

$$CrCl_2 \xrightarrow[\text{THF, room temp, 3 h in the dark}]{\text{1\% Na/Hg, 6CN-}t\text{-C}_4\text{H}_9} \underset{1,\ 69\%}{[Cr(CN\text{-}t\text{-}C_4H_9)_6]} \quad (3)$$

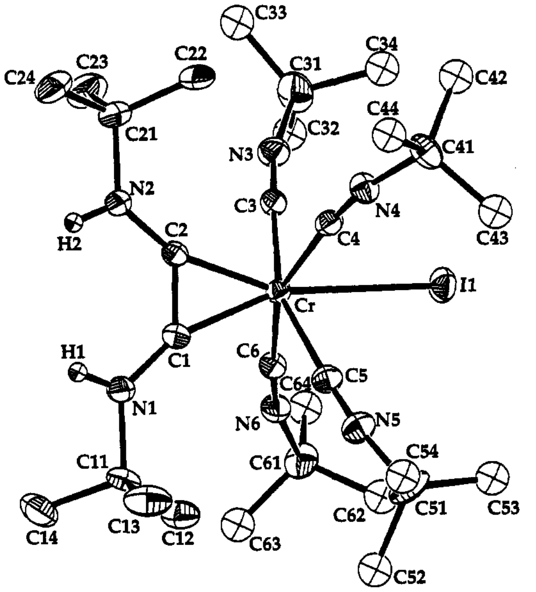

Figure 3. ORTEP diagram of [Cr(t-C_4H_9HNC≡CNH-t-C_4H_9)(CN-t-C_4H_9)$_4$I]$^+$, showing the atom labeling scheme and the 40% probability ellipsoids. The methyl carbons on C3–C6 are represented as 3-Å^2 isotropic spheres for clarity.

An ORTEP diagram of one of the molecules in the asymmetric unit of 1 is shown in Figure 1. Final positional and thermal parameters and selected bond distances and angles are summarized in Tables 2 and 3, respectively. Compound 1 is isomorphous and isostructural with [Mo-(CN-t-C_4H_9)$_6$],[6] differing only in the nature of the *tert*-butyl group disorder. The geometry at the Cr center is approximately octahedral. As in the case of [Mo(CN-t-C_4H_9)$_6$], the most notable feature of the structure is the variety of isocyanide ligand bend angles, ranging from severely bent, 136.1(9)° for C13–N13–C131, to nearly linear, 175(1)° for C23–N23–C231. The average bending angle for the 12 crystallographically independent isocyanide ligands is 153°, a value indicative of a highly electron rich Cr center donating π electrons to the ligands. This phenomenon is well-known for low valent metal isocyanide complexes and is also postulated to promote the reductive coupling reaction by increasing the electrophilicity of the isocyanide ligands, as discussed previously.[6] As illustrated in Figure 2, there is an approximately linear relationship between the isocyanide ligand C–N–C angles and the corresponding metal–carbon bond lengths for [Mo(CN-t-C_4H_9)$_6$] and 1. This relationship reflects the resonance structures **I** and **II**. Figure 2 further reveals that [Cr-($CNCF_3$)$_6$] behaves similarly,[15] but the aromatic homoleptic analogs exhibit less bending of the C–N–C angles because of resonance structures **III**.

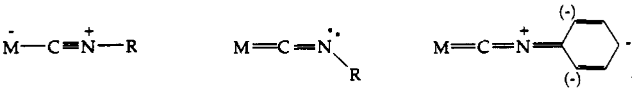

I II III

Table 4. Final Positional Parameters and *B*(eq) for $[\mathrm{Cr}(t\text{-}\mathrm{C_4H_9HNC{\equiv}CNH}\text{-}t\text{-}\mathrm{C_4H_9})(\mathrm{CN}\text{-}t\text{-}\mathrm{C_4H_9})_4\mathrm{I}]\mathrm{I}\cdot(\text{toluene})$ (2·(toluene))[a]

atom	*x*	*y*	*z*	B_{eq}, Å² [b]
I1	0.13384(2)	0.67698(2)	0.80548(2)	2.92(1)
I2	0.17263(3)	0.76435(2)	0.34591(3)	5.09(2)
Cr1	0.03686(4)	0.53465(4)	0.76495(4)	1.73(2)
N1	−0.1436(2)	0.4336(2)	0.7231(2)	2.3(2)
N2	0.0294(3)	0.3553(2)	0.7193(2)	2.3(1)
N3	0.2243(2)	0.4845(2)	0.8939(2)	2.8(2)
N4	0.1108(2)	0.5537(2)	0.6220(2)	2.4(1)
N5	−0.1062(3)	0.6486(2)	0.6498(2)	3.0(2)
N6	−0.0074(2)	0.5930(2)	0.9169(2)	2.5(1)
C1	−0.0621(3)	0.4616(2)	0.7380(2)	1.9(2)
C2	0.0147(3)	0.4267(2)	0.7380(2)	1.8(2)
C3	0.1547(3)	0.5009(2)	0.8453(3)	2.0(2)
C4	0.0854(3)	0.5425(2)	0.6751(3)	2.1(2)
C5	−0.0553(3)	0.6059(2)	0.6937(3)	2.3(2)
C6	0.0072(3)	0.5681(2)	0.8617(3)	2.2(2)
C11	−0.2294(3)	0.4718(3)	0.7172(3)	2.7(2)
C12	−0.2130(3)	0.5406(3)	0.7730(3)	3.3(2)
C13	−0.2784(3)	0.4936(4)	0.6271(3)	4.3(2)
C14	−0.2846(3)	0.4119(3)	0.7425(4)	4.2(2)
C21	0.1145(3)	0.3169(3)	0.7253(3)	2.8(2)
C22	0.1737(3)	0.3698(3)	0.6981(3)	3.5(2)
C23	0.1633(4)	0.2906(3)	0.8141(4)	4.4(2)
C24	0.0878(4)	0.2469(3)	0.6683(4)	4.2(2)
C31	0.3163(3)	0.4844(3)	0.9541(4)	4.5(2)
C32	0.3122(5)	0.5033(6)	1.0372(5)	9.0(4)
C33	0.3561(4)	0.4056(4)	0.9562(6)	8.8(4)
C34	0.3664(4)	0.5470(4)	0.9292(5)	7.8(4)
C41	0.1469(3)	0.5861(3)	0.5623(3)	3.2(2)
C42	0.2474(4)	0.5847(4)	0.6021(4)	5.8(3)
C43	0.1138(5)	0.6693(4)	0.5482(4)	6.0(3)
C44	0.1116(5)	0.5406(5)	0.4842(4)	6.8(4)
C51	−0.1600(4)	0.7125(3)	0.6041(4)	4.1(2)
C52	−0.2421(7)	0.7189(5)	0.6298(7)	11.6(6)
C53	−0.1045(7)	0.7822(4)	0.6282(7)	13.2(6)
C54	−0.1912(7)	0.6948(5)	0.5165(5)	10.1(5)
C61	−0.0172(4)	0.6420(3)	0.9811(3)	3.2(2)
C62	−0.0295(6)	0.7228(3)	0.9488(5)	6.8(4)
C63	−0.0973(4)	0.6146(4)	1.0004(4)	4.8(3)
C64	0.0680(4)	0.6307(4)	1.0571(4)	5.9(3)
C100	−0.0037(6)	0.1208(5)	0.8787(6)	10.0(5)
C101	0.0177(4)	0.0462(4)	0.8504(4)	5.1(3)
C102	0.0058(4)	0.0356(4)	0.7686(4)	4.9(3)
C103	0.0278(5)	−0.0336(6)	0.7426(5)	7.2(4)
C104	0.0591(6)	−0.0916(5)	0.7969(9)	9.5(5)
C105	0.0709(6)	−0.0847(7)	0.8762(8)	10.4(6)
C106	0.0501(5)	−0.0140(6)	0.9039(5)	7.0(4)
H1	−0.152(3)	0.388(2)	0.710(2)	1.2(9)
H2	−0.014(3)	0.324(3)	0.707(3)	3(1)

[a] Numbers in parentheses are estimated standard deviations of the last significant figure. See Figure 3 for the atom labeling scheme. [b] $B_{eq} = {}^4/_3[a^2\beta_{11} + b^2\beta_{22} + c^2\beta_{33} + 2ab\cos(\gamma)\beta_{12} + 2ac\cos(\beta)\beta_{13} + 2bc\cos(\alpha)\beta_{23}]$.

Table 5. Selected Interatomic Distances (Å) for $[\mathrm{Cr}(t\text{-}\mathrm{C_4H_9HNC{\equiv}CNH}\text{-}t\text{-}\mathrm{C_4H_9})(\mathrm{CN}\text{-}t\text{-}\mathrm{C_4H_9})_4\mathrm{I}]^+$ [a]

Cr–I1	2.8670(8)	N1–C11	1.488(5)
Cr–C1	1.944(4)	N2–C21	1.481(5)
Cr–C2	1.937(4)	C3–N3	1.159(5)
Cr–C3	1.976(4)	C4–N4	1.149(5)
Cr–C4	1.982(5)	C5–N5	1.157(5)
Cr–C5	1.974(4)	C6–N6	1.149(5)
Cr–C6	1.989(5)	N3–C31	1.457(6)
C1–C2	1.367(6)	N4–C41	1.468(6)
C1–N1	1.321(5)	N5–C51	1.451(6)
C2–N2	1.326(5)	N6–C61	1.451(6)
N1–H1	0.82(4)	mean C–C(methyl)	1.51(2)[b]
N2–H2	0.85(5)	range C–C(methyl)	1.451(9)–1.53(1)

[a] See footnote *a*, Table 4. [b] Numbers in parentheses are the standard deviations of the mean.

Addition of 2 equiv of HI to a THF solution of 1 resulted in the reductive coupling of two adjacent isocyanide ligands to produce $[\mathrm{Cr}(t\text{-}\mathrm{C_4H_9HNC{\equiv}CNH}\text{-}t\text{-}\mathrm{C_4H_9})(\mathrm{CN}\text{-}t\text{-}\mathrm{C_4H_9})_4\mathrm{I}]\mathrm{I}$ (2), as indicated in eq 4. The best results were obtained when the reaction solution was purified by passage through silica gel before evaporating the solvent, presumably to remove traces of water remaining from the aqueous acid. The relatively air-stable product decomposes over time in

Table 6. Selected Bond Angles (deg) for $[\mathrm{Cr}(t\text{-}\mathrm{C_4H_9HNC{\equiv}CNH}\text{-}t\text{-}\mathrm{C_4H_9})(\mathrm{CN}\text{-}t\text{-}\mathrm{C_4H_9})_4\mathrm{I}]\mathrm{I}^+$ [a]

I1–Cr–C1	160.1(1)	C5–Cr–C6	89.7(2)
I1–Cr–C2	158.6(1)	Cr–C1–N1	160.2(3)
I1–Cr–C3	78.2(1)	Cr–C2–N2	159.2(3)
I1–Cr–C4	78.7(1)	Cr–C3–N3	176.8(4)
I1–Cr–C5	79.8(1)	Cr–C4–N4	173.9(4)
I1–Cr–C6	79.2(1)	Cr–C5–N5	176.4(4)
C1–Cr–C2	41.2(2)	Cr–C6–N6	174.7(4)
C1–Cr–C3	117.0(2)	C1–C2–N2	130.9(4)
C1–Cr–C4	111.7(2)	C2–C1–N1	130.7(4)
C1–Cr–C5	84.7(2)	C1–N1–C11	131.3(4)
C1–Cr–C6	88.5(2)	C2–N2–C21	130.0(4)
C2–Cr–C3	85.7(2)	C1–N1–H1	117(3)
C2–Cr–C4	88.0(2)	C2–N2–H2	118(3)
C2–Cr–C5	115.4(2)	C11–N1–H1	111(3)
C2–Cr–C6	114.2(2)	C21–N2–H2	112(3)
C3–Cr–C4	91.9(2)	C3–N3–C31	165.5(5)
C3–Cr–C5	158.0(2)	C4–N4–C41	166.7(4)
C3–Cr–C6	87.0(2)	C5–N5–C51	169.9(5)
C4–Cr–C5	83.0(2)	C6–N6–C61	165.7(4)
C4–Cr–C6	157.6(2)		
range N–C–C (methyl)		range C(methyl)–C–C(methyl)	
groups 1 and 2	106.3(4)–111.8(4)	groups 1 and 2	109.4(4)–111.6(4)
groups 3–6	106.0(4)–108.8(5)	groups 3–6	108.5(7)–114.4(8)
mean N–C–C (methyl)		mean C(methyl)–C–C(methyl)	
groups 1 and 2	109(2)[b]	groups 1 and 2	110.2(8)[b]
groups 3–6	108(1)[b]	groups 3–6	111(2)[b]

[a] Estimated standard deviations in the least significant figure are given in parentheses. [b] Numbers in parentheses are the standard deviations of the mean.

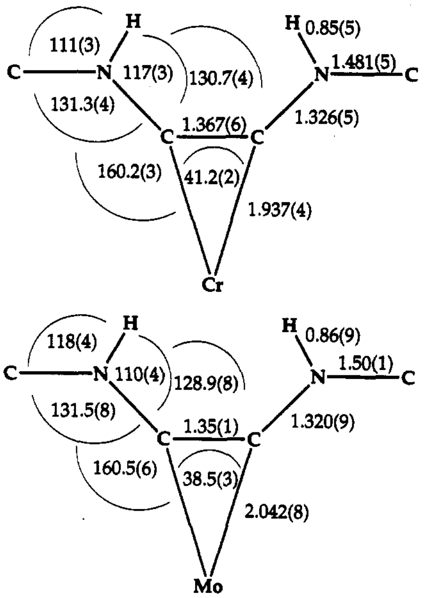

Figure 4. Comparison of the bond distances and angles about the cores of $[\mathrm{Cr}(t\text{-}\mathrm{C_4H_9HNC{\equiv}CNH}\text{-}t\text{-}\mathrm{C_4H_9})(\mathrm{CN}\text{-}t\text{-}\mathrm{C_4H_9})_4\mathrm{I}]\mathrm{I}$ (2) and the corresponding molybdenum coupled product, $[\mathrm{Mo}(t\text{-}\mathrm{C_4H_9HNC{\equiv}CNH}\text{-}t\text{-}\mathrm{C_4H_9})(\mathrm{CN}\text{-}t\text{-}\mathrm{C_4H_9})_4\mathrm{I}]\mathrm{I}$. Numbers in parentheses are estimated standard deviations in the last significant figure.

$$\underset{\mathbf{1}}{[\mathrm{Cr(CN}\text{-}t\text{-}\mathrm{C_4H_9)_6}]} \xrightarrow[\text{THF, room temp, 1 h}]{\text{2HI (aq, 57\%)}} \underset{\mathbf{2},\ 86\%}{[\mathrm{Cr}(t\text{-}\mathrm{C_4H_9NHC{\equiv}CNH}\text{-}t\text{-}\mathrm{C_4H_9})(\mathrm{CN}\text{-}t\text{-}\mathrm{C_4H_9})_4\mathrm{I}]\mathrm{I}} \quad (4)$$

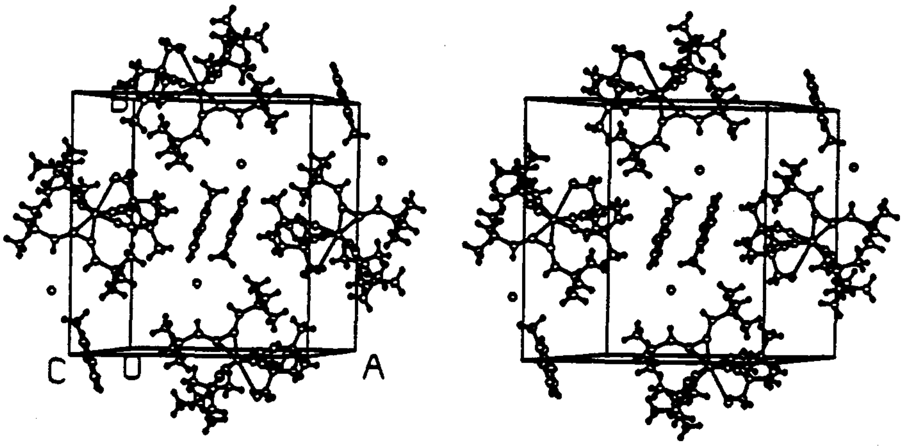

Figure 5. Packing diagram in stereoview of [Cr(t-C_4H_9HNC$\equiv$CNH-t-C_4H_9)(CN-t-C_4H_9)$_4$I]I·(toluene) (**2**·(toluene)). Hydrogen atoms and solvent molecules (toluene) are included.

the presence of water. The coupled product **2** was identified by its IR, ^{1}H NMR, and ^{13}C{^{1}H} NMR spectra. A strong peak at 1604 cm^{-1} in the infrared spectrum is indicative of a metal-coordinated acetylene ligand of the form (RHNC$\equiv$CNHR). Bands at 3151 and 3106 cm^{-1}, arising from N—H stretching modes, further indicate coupled product formation. The ^{1}H NMR spectrum supports these assignments. Peaks at 1.43, 1.74, and 10.51 ppm in a ratio of 18:9:2 can be assigned, respectively, to *tert*-butyl protons on linear (CN-t-C_4H_9) ligands, *tert*-butyl protons on the bound acetylene, and N—H protons. Further support for a bound acetylene is provided by a resonance in the ^{13}C NMR spectrum at 209 ppm. Definitive structural proof in the solid state was provided by the X-ray diffraction study.

An ORTEP diagram of the cation of **2** is shown in Figure 3. Final positional and thermal parameters, selected bond distances, and bond angles for **2**·(toluene) are summarized in Tables 4–6, respectively. The Cr center has idealized C_{2v} capped trigonal prismatic geometry, taking the bound acetylene to occupy two coordination sites. The core structure is very similar to that of the molybdenum analog, [Mo(t-C_4H_9HNC$\equiv$CNHt-C_4H_9)(CN-t-C_4H_9)$_4$I]I.[17] The metrical parameters of the coupled ligands in the two are compared in Figure 4, which reveals some noteworthy differences. The metal—carbon distance is 0.11 Å shorter in **2** than in the molybdenum analog, corresponding to the differences in their atomic radii [Cr(0) = 1.29 Å; Mo(0) = 1.40 Å].[18] This difference in turn produces a slightly larger C1—Cr—C2 angle (approximately 3°) in **2**. Figure 5 shows a packing diagram of **2**·(toluene), salient features of which are the close contacts between the ionic iodide I2 and the N—H protons on the coordinated aminoacetylene ligand, I2···N1 = 3.613(4) Å (I2···H1 = 2.560 Å) and I2···N2 = 3.646(4) Å (I2···H2 = 2.721 Å). This interaction was also observed in the lattice structure of [Mo(t-C_4H_9HNC$\equiv$CNH-t-C_4H_9)(CN-t-C_4H_9)$_4$I]I, I2···N2 = 3.72 Å (I2···H1 = 3.05 Å) and I2···N2 = 3.68 Å (I2···H2 = 2.81 Å).

As reported for [Mo(t-C_4H_9HNC$\equiv$CNH-t-C_4H_9)(CN-t-C_4H_9)$_4$I]I,[5] removal of the coupled ligand from **2** with the C—C bond intact could be accomplished oxidatively (eq 5). Addition of excess H_2O_2 to [Cr(t-C_4H_9HNC$\equiv$CNH-t-C_4H_9)(CN-t-C_4H_9)$_4$I]I (**2**) in THF resulted in the formation of a product with a retention time and mass spectrum by GC/MS analysis identical to those of a genuine sample of *N*,*N*′-di-*tert*-butyloxamide.[5] The 28% yield of oxamide achieved from this oxidation was comparable to those reported previously from oxidations of [Mo(t-C_4H_9HNC$\equiv$CNH-t-C_4H_9)(CN-t-C_4H_9)$_4$I]I.

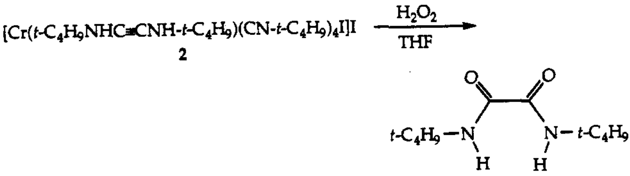

(5)

Conclusions

A convenient synthesis of [Cr(CN-t-C_4H_9)$_6$] (**1**) has been reported. The structural characterization of this compound augments the small body of X-ray diffraction studies of homoleptic Cr(0) isocyanide compounds. The large bend angles of the CNR groups in this molecule indicate a highly electron dense metal center, as was seen earlier for [Mo(CN-t-C_4H_9)$_6$], and attest to its propensity to undergo reductive coupling. A linear relationship between M–CNR distances and MC–N–R bend angles was found. Reductive coupling of two isocyanide ligands of **1** upon addition of 2 equiv of HI afforded [Cr(t-C_4H_9HNC$\equiv$CNH-t-C_4H_9)(CN-t-C_4H_9)$_4$I]I (**2**). This reaction extends the reductive coupling reaction of isocyanide ligands to a first row transition metal. A crystal structure of **2** revealed its similarity to the analogous coupled product [Mo(t-C_4H_9HNC$\equiv$CNH-t-C_4H_9)(CN-t-C_4H_9)$_4$I]I. Oxidative removal of the coupled ligand from **2** as the corresponding di-*tert*-butyloxamide was also achieved.

Acknowledgment. This work was supported by a grant from the National Science Foundation. We thank Drs. E. M. Carnahan and J. D. Protasiewicz for helpful discussions.

Supplementary Material Available: Tables of anisotropic temperature factors (Tables S1, S4), complete bond distances (Table S2, S5), and bond angles (Table S3, S6) for complexes **1** and **2**, respectively (14 pages). Ordering information is given on any current masthead page.

OM930765Y

---

[17] Corfield, P. W. R.; Baltusis, L. M.; Lippard, S. J. *Inorg. Chem.* **1981**, *20*, 922.

[18] Wells, A. F. *Structural Inorganic Chemistry*; Oxford University Press: Oxford, U.K., 1984.